Available online at www.sciencedirect.com

Manufacturing Letters

Manufacturing Letters 33 (2022) 786–793

50th SME North American Manufacturing Research Conference (NAMRC 50, 2022)

A machining digital twin for hybrid manufacturing

Jake Dvorak[a], Aaron Cornelius[a], Greg Corson[a], Ross Zameroski[a], Leah Jacobs[a], Joshua Penney[a], Tony Schmitz[a,b,*]

[a]*University of Tennessee, Knoxville, Mechanical, Aerospace, and Biomedical Engineering Department, Knoxville, Tennesse, USA*
[b]*Oak Ridge National Laboratory, Manufacturing Science Division, Oak Ridge, Tennessee, USA*

* Corresponding author. Tel.: +1-865-974-6141. *E-mail address:* tony.schmitz@utk.edu

Abstract

Hybrid manufacturing consisting of metal additively manufactured preforms and computer numerical control (CNC) machining has been established to be an effective method for high material use rates. However, hybrid manufacturing introduces unique challenges. Near-net shape designs are typically selected, which result in a smaller margin for part placement within the stock and stringent requirements for work coordinate system identification. Additionally, less stock material reduces the preform stiffness, which limits the material removal rates during machining. This paper demonstrates a digital twin for CNC machining of a wire arc additively manufactured preform that implements: 1) structured light scanning for stock model identification and tool path generation; 2) a fused filament fabrication apparatus to attach temporary fiducials and scan targets to the preform that enable coordinate system definition for both the CAM and CNC machine; 3) preform and tool tip frequency response function measurements to enable stable milling parameter selection; and 4) post-manufacturing measurements of geometry, surface finish, and structural dynamics to confirm designer intent. These efforts define key components of the machining digital twin for hybrid manufacturing.

Keywords: Wire arc additive manufacturing; milling; hybrid manufacturing; fiducial; structured light scanning; machining dynamics

1. Introduction

The key topics of this research effort are hybrid manufacturing and the associated digital twin. While many digital twin descriptions are available, for the purposes of this study the working definition is: the digital counterpart, or twin, of a physical process that uses models and real-time data to predict the behavior of the physical process [1-8]. While real-time data is an important component of the digital twin, pre- and in-process discrete measurements and predictive process models are also critical. The focus of this paper is the latter.

Hybrid manufacturing encompasses a sequence of activities that integrate additive manufacturing (AM) with other processes. Here, AM + metrology + machining activities are used to produce the final part with geometry and surface finish that meet the designer's intent. The digital twin for this particular application of hybrid manufacturing includes:

- the AM material, parameters, and path used to fabricate the preform
- in-process print data, such as temperature maps and surface images
- the preform geometry
- the preform structural dynamics
- the cutting tool-holder-spindle-machine structural dynamics
- a physics-based model to relate the preform material's cutting force model, preform and tool-holder-spindle-machine structural dynamics, and milling stability [9]
- the machining parameters and toolpaths
- the final part geometry and surface finish of the machined part.

In this research, the focus is the digital twin information associated with the machining steps. This includes: 1) a structured light scan of the AM preform with temporary

fiducials used to identify a local coordinate system; 2) selection of the cutting tool used to machine the preform; 3) measurements of the tool-holder-spindle-machine and preform frequency response functions, or FRFs, which describe their vibration behavior; 4) the milling parameters, which include the axial and radial depths of cut, spindle speed, and feed per tooth values; 5) the toolpaths generated by the computer-aided manufacturing (CAM) software; and 6) the machined part geometry, surface finish, and structural dynamics.

Collectively, these data and models provide a digital counterpart to the physical manufacturing process that includes: the actual AM part geometry with a local coordinate system that can be identified on the machine using standard probing cycles, transfer of that coordinate system to the CAM software via an accurate stock model, selection of machining parameters using the structural dynamics and physics-based milling stability model, and assessment of the machining outcome by post-process measurements. For the purposes of demonstrating these steps a wire arc additive manufacturing (WAAM) wall-shaped preform was printed on a steel baseplate; see Fig. 1.

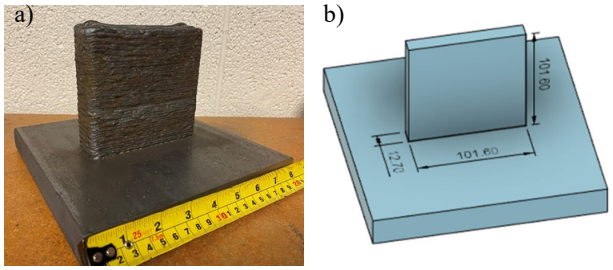

Fig. 1. (a) Wall preform as printed on a baseplate; (b) wall and baseplate as modeled (dimensions in mm).

The paper is organized as follows. First, a review of prior efforts for hybrid manufacturing, structured light scanning, and fiducial use is provided. Second, a description of temporary fiducials for preform measurement and coordinate system identification is given. Third, the use of a structured light scan to provide a CAM stock model is detailed. Fourth, the measurement of the tool-holder-spindle and preform structural dynamics and the corresponding milling parameter selection and machining performance are discussed. Fifth, the machined part measurements are described. Finally, a discussion of the results and conclusions are provided.

2. Prior Research

Webster *et al*. recently defined hybrid manufacturing as an "in-situ or series combination of an additive manufacturing process and secondary energy sources in which physical mechanisms are fundamentally altered/controlled to affect the resulting properties of the material and/or part" [10]. They include an "AM + X" convention that describes AM plus a secondary process (e.g., milling). Liou *et al*. described a case of powder-based laser metal deposition + CNC milling in a single machine [11]. They defined an automated process planning sequence composed of determining the base face (which functioned as the machining fixture), extracting the part skeleton, decomposing a part into subparts, determining build sequence and direction for subparts, checking the feasibility of the build sequence and direction for the machining process, and optimization of the deposition and machining steps. Yamazaki described the combination of laser metal deposition, turning, and milling capabilities in a single, commercial machine [12]. Advantages were increased functionality and flexibility for small lot production runs. Disadvantages include heat transfer into the machine structure from the laser deposition, which can limit accuracy, and the combination of powder (for deposition) and coolant (for machining) in the same work volume. Song *et al*. explored early process development of WAAM + CNC milling in a single machine [13]. They described a retrofit of gas metal arc welding (GMAW) on a three-axis milling machine to enable both high-rate deposition and material removal to obtain the required surface finish. The setup included a heated build plate to reduce residual stress during deposition.

Structured light scanning systems use a projector to shine a structured pattern onto the test object. One or more cameras capture the reflected, distorted pattern from the test object. The geometric shape of the object is obtained using the distorted pattern and the scanner's calibration. Structured light has become a well-established instrument for manufacturing environment measurements [14]. Mendricky used an artifact containing multiple precision spheres and determined accuracy of sphere diameters and distances from an optical scanner by comparing results to a coordinate measuring machine [15]. Most of the defined parameter results showed the accuracy of the optical scanner as comparable to the coordinate measure machine or within an order of magnitude.

Fiducials are commonly used in manufacturing to complete machine calibration or part location [16-18]. Smith *et al*. demonstrated the fiducial calibration system (FCS) by attaching fiducials to a large, monolithic workpiece, measuring in a metrology environment, and remeasuring in the manufacturing environment. The accuracy of a coordinate measuring machine can be transferred to the machine tool via a transformation of the CNC program coordinates such that the machine features were correct regardless of the manufacturing environment and machine tool errors [19-20].

Cornelius *et al*. described the temporary fiducial approach using a friction stir additive part and CNC machining [21]. They focused on the methodology of defining and transferring coordinate systems through hybrid manufacturing operations. Their approach was implemented here. In related efforts, Luo *et al*. proposed a digital twin for CNC machine tools to reduce failure probability and improve stability [22]. Zhou *et al*. introduced "a knowledge-driven digital twin manufacturing cell, which aims to maximize the product quality and throughput, while keeping flexibility and reducing cost, by an intelligent perceiving, simulating, understanding, predicting, optimizing and controlling strategy" [23]. They stated that a digital twin is one of three enabling technologies for this strategy.

3. External Fiducial Apparatus

An external fiducial apparatus was designed and fabricated using fused filament fabrication (FFF) with ABS material. The apparatus volume was small to limit material use and avoid obscuring the preform during scanning, while remaining generic for use with various preform geometries. The fiducial apparatus serves two major purposes. First, it supports fiducials (tooling spheres in this case) that can be located in both the scan and in the milling machine. Second, it supports targets that the scanning software requires to maintain tracking across scans. Therefore, targets are not needed on the build plate or part itself. The fiducial apparatus was attached via two threaded fasteners on both the left and right side of the baseplate; see Figure 2. The left fiducial apparatus contained two spheres while the right contained only one sphere (not shown in Fig. 2).

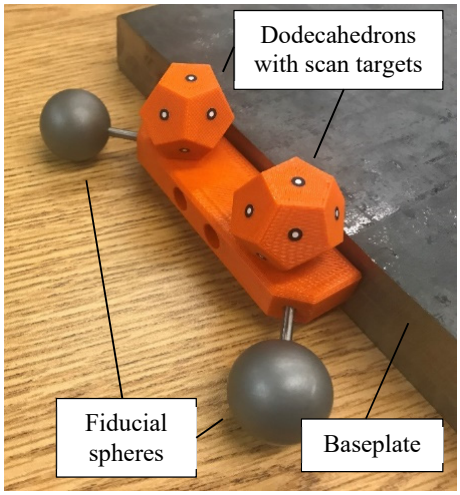

Fig. 2. External fiducial apparatus that supports the fiducials (25.4 mm diameter, satin-finish spheres) and dodecahedron scan targets. The fiducial apparatus was attached to baseplate using threaded fasteners.

The fiducials were 25.4 mm diameter satin-finish spheres designed for optical scanning calibration (Bal-tec SAT-B100). The spheres were attached to the apparatus using press-fit dowel pins. Because it is necessary for the spheres to be accessible to both the structured light scanner (line-of-sight imaging) and the spindle-mounted probe on the milling machine, the fiducial apparatus was designed to hold the fiducials at a 45-deg angle to maximize probe access. It was not necessary to specifically locate the spheres on the baseplate or relative to the preform because their positions are measured together with the part geometry using the structured light scanner.

The scanning targets were placed on the faces of two dodecahedrons per fiducial apparatus (four total). The dodecahedron was chosen to provide multiple faces/targets at any viewing angle. The structured light scanning system used in this research (GOM ATOS Q) requires at least three targets to be in view from one scan to the next.

4. Scan to CAM

An initial scan of the preform with fiducials is displayed in Fig. 3. The computer-aided design (CAD) digital preform model was aligned to the scan using the three planes of the base plate. The final alignment of the scan to preform model is also shown in Fig. 3. This alignment was used to visually ensure that the preform model was fully contained within the scan (as-printed preform). The WAAM preform was intentionally overbuilt by approximately 8 mm is all directions.

After the preform scan and model were aligned, the shared coordinate system was established. The coordinate system was defined kinematically based on a series of best-fit primitives [21, 24]. The center of the first sphere was selected as the part origin, fixing three translational degrees of freedom. The bottom of the build plate defined the Z axis, fixing two rotational degrees of freedom. The line between the centers of the first and second spheres (left and right front spheres in Fig. 3) defined the X axis, fixing the final rotational degree of freedom. The third sphere was redundant due to the build plate geometric constraint and was not used to define the coordinate system. The coordinate system is displayed at the left front sphere in Fig. 3.

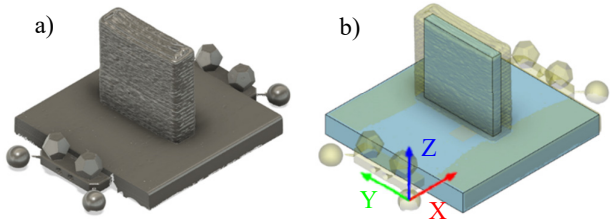

Fig. 3. (a) Scan of wall with attached fiducials; (b) Alignment of wall geometry inside the preform.

Toolpaths were then defined relative to the established coordinate system within Fusion 360, the CAM software; see Fig. 4. The scan was imported directly as the CAM stock model to enable full digital simulation. A screenshot of the simulation is also shown in Fig. 4. This simulation, again, provided verification that the model was fully contained within the preform. The accurate stock model enabled collision detection and provided the actual surface location for setting the initial radial depth of cut to engage the endmill by the desired amount into the rough WAAM surface.

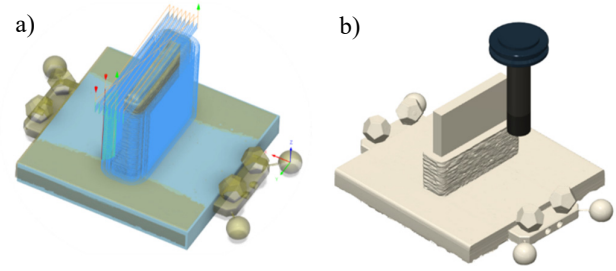

Fig. 4. (a) CAM toolpaths for wall machining; (b) CAM simulation of wall machining.

The preform was then loaded into a Haas VF-4 three-axis CNC milling machine and clamped to the table using a vise; this aligned the bottom of the baseplate to the machine table and defined the Z axis direction. To fully relate the preform and machine coordinate systems, two tooling spheres (left and right front spheres in Fig. 3) were probed using the on-machine touch trigger probe (Renishaw OMP40-2) and built-in routines to find the sphere centers. The line between the two front sphere centers described the preform's X axis. A coordinate rotation about the Z axis was then performed to align the machine X direction with the preform X direction. No probing of the preform was required since the tooling spheres were already related to the preform location in the scan and, therefore, the CAM stock model used to generate the toolpaths.

5. Machining Dynamics/Milling Parameter Selection

A four flute, coated, carbide, 25.4 mm diameter end mill with a 25.4 mm flute length (YG1 model UGMF73912) was used to machine the preform. The endmill had a 103 mm extension length from the tool holder and had a reduced shank diameter to enable machining of the full wall height. Mobilcut 100, a diluted oil-based soluble coolant was used during the machining process. To determine optimum milling parameters a tap test was performed both at the tool's free end and the preform's top corner (perpendicular to the preform faces) to measure the frequency response functions, or FRFs; see Figures 5 and 6.

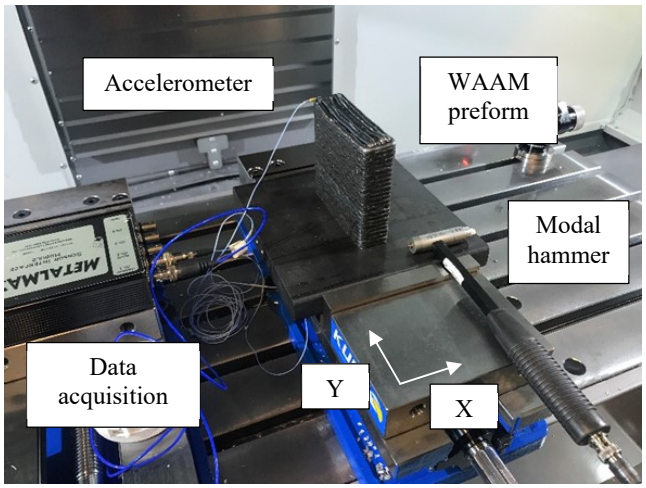

Fig. 5. Preform tap testing setup.

Figure 6 shows that the tool was much less stiff (i.e., larger amplitudes in the real and imaginary parts of the complex-valued FRFs) than the preform and therefore dominated the selection of stable milling parameters. The tool and preform FRFs were then used to generate the corresponding stability maps (Fig. 7), where the specific cutting force for the steel preform was 1985 N/mm^2 [9]. The stability map calculations were based on a frequency-domain stability analysis that incorporates the tool tip FRF and force model [9]. Given the stability map, which provides a digital model for the milling process behavior, an initial axial depth of cut of 2 mm and spindle speed of 5300 rpm were selected to obtain stable

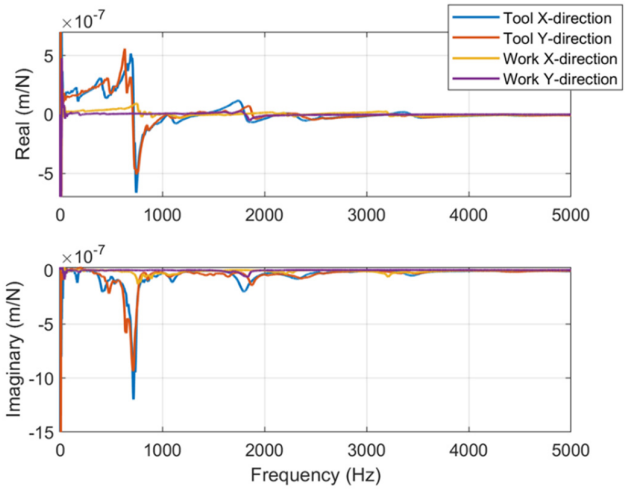

Fig. 6. Real (top panel) and imaginary (bottom panel) parts of the tool and preform FRFs in the X and Y directions.

(chatter-free) cutting conditions. The corresponding surface speed was 422.9 m/min and the feed per tooth was 0.026 mm.

The machining process consisted of two primary operations completed in a single setup with down milling. First, the preform top was faced. Second, the sides were machined. The top facing nominally consisted of four axial steps down; however, an extra step was added due to a visual discovery of excessive internal voids created by the WAAM process. This reduced the wall's final height by 2 mm. The side milling operations included three radial steps: 3.05 mm radial depth to clean up the preform's initial rough surface; 5.08 mm to remove the bulk of the material; and 2.54 mm for the final pass. Photographs of the preform after facing the top and completing a few axial steps down the sides are provided in Fig. 8.

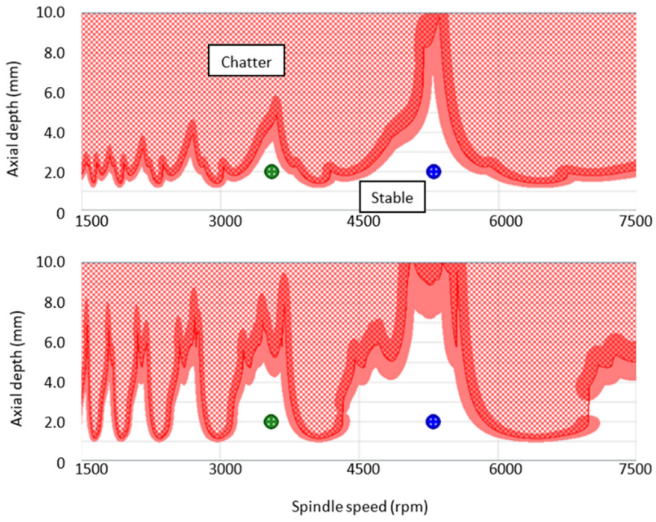

Fig. 7. Stability maps for X direction milling (top panel) and Y direction milling (bottom panel). The blue marker designates the parameters for the initial 10 mm of material removal (near the preform top). The green marker designates the parameters for the remaining height. The red shaded region indicates combinations with uncertainty.

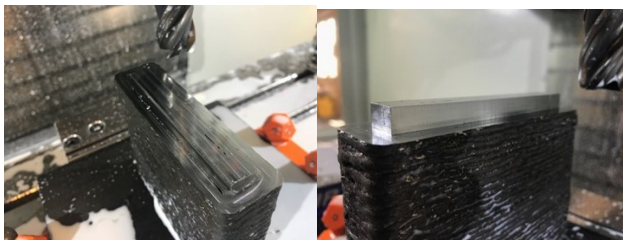

Fig. 8. Photographs during preform milling.

At a height of 10 mm from the preform top, the spindle speed was reduced to 3550 rpm in the next lowest lobe since initial wear was visually observed on the endmill when periodically pausing in-between passes. The reduced cutting speed (283.3 m/min) decreased the wear rate and enabled the wall to be finished, while retaining stable cutting conditions. Feed rate was left unchanged. This second selected point is identified in the Fig. 7 stability maps. A final shallow axial depth of cut pass was done to ensure the entire wall height was machined and the baseplate was cut into.

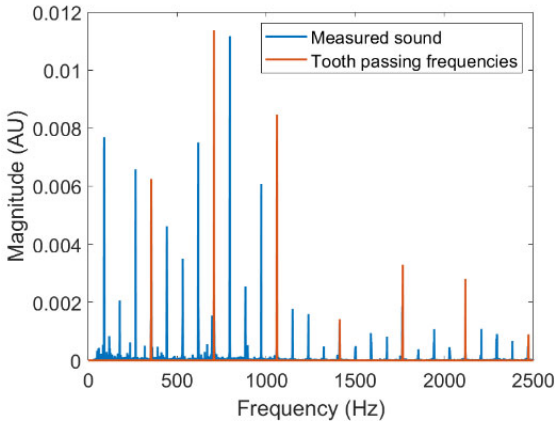

Fig. 9. Frequency content of sound signal measured during milling for the preform top, 5300 rpm.

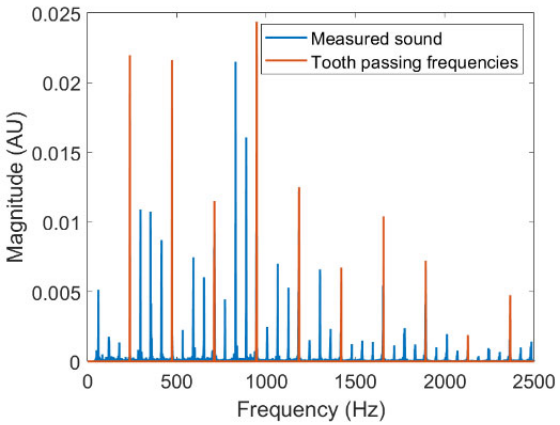

Fig. 10. Frequency content of sound signal measured during milling for the preform middle, 3550 rpm.

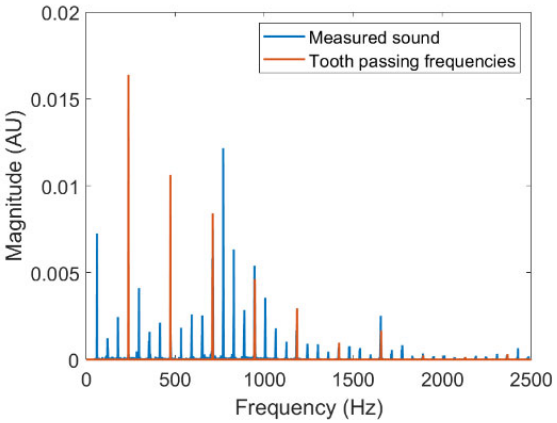

Fig. 11. Frequency content of sound signal measured during milling for the preform bottom, 3550 rpm.

To verify that the machining conditions were stable, audio data was recorded during machining and the frequency content was evaluated after machining. Measurements from the beginning (near the preform top), middle, and end (near the preform bottom) of the side milling processes are provided in Figs. 9-11. The fast Fourier transform was performed on audio data parsed to the steady state cutting condition (avoiding entry and exit of the cut). In these instances, the cutting sound dominated the ambient or white noise, therefore no filtering was required. It is observed that the measured sound occurs at the tooth passing frequency (spindle speed multiplied by the number of teeth), integer multiples of the tooth passing frequency, or runout frequencies (spindle speed and its integer multiples). These observations are indicative of a stable machining process, as unstable machining would show dominant frequency content that does not align with the tooth passing and runout frequencies, in general. A photograph of the wall after machining is displayed in Fig. 12.

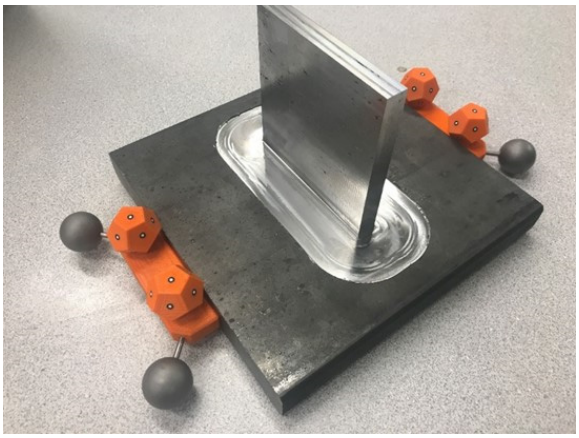

Fig. 12. Wall geometry after milling. The fiducials are still attached to the baseplate.

6. Post-machining measurements

Measurements were completed after machining to verify the geometry and surface finish of the wall. First, a scan was completed of the wall with the fiducials still attached. A surface deviation plot was generated to compare the machined part to

the CAD model; see Fig. 13. Note that the top of the wall shows a larger error due to the additional facing step completed at the wall top (not originally modeled in CAD). Other significantly negative values are due to voids left by the WAAM process. Positive readings are attributed to tool wear, which exceeded 0.6 mm flank wear width at the end of the cut; see Fig. 14.

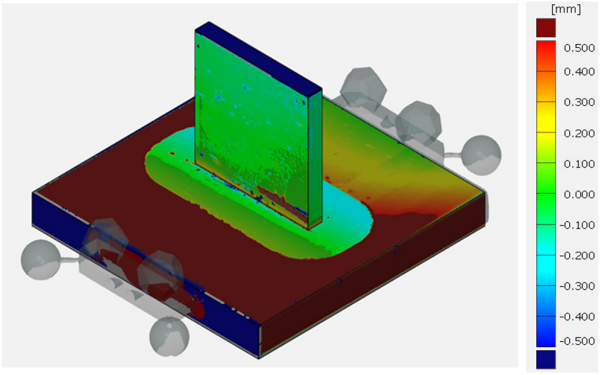

Fig. 13. Surface deviations between the as-machined scan and the CAD model. "Front" refers to the face pointing towards two fiducial spheres, and "back" towards a single fiducial sphere.

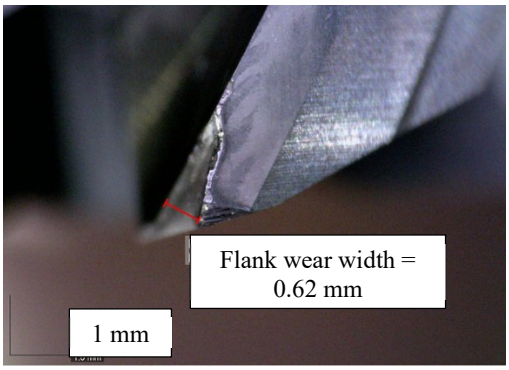

Fig. 14. Tool wear on the flank face of the most worn cutting edge after machining.

A Mitutoyo Surftest SJ-210 stylus profilometer was used to further examine the machined surface. The SJ-210 contained a stylus with a 2 µm radius tip, a 60 degree tip angle, and 0.75 mN of measuring force. Average roughness (Ra) measurements were performed in the feed direction (Y in Figure 5) at various Z heights in the YZ plane; see Figure 15. The ISO 1997 standard was used in conjunction with Gaussian filtering with a 0.25 mm cutoff, wavelength of 2.5 µm, and cutoff number of 9. These Ra values agree with the simulated average roughness of 0.4 µm for the selected feed per tooth. The simulation was based on numerical solution of the second-order, delay differential equations of motion that describe the milling process. It included the cycloidal motion of the cutter teeth to accurately simulate the machined surface [9].

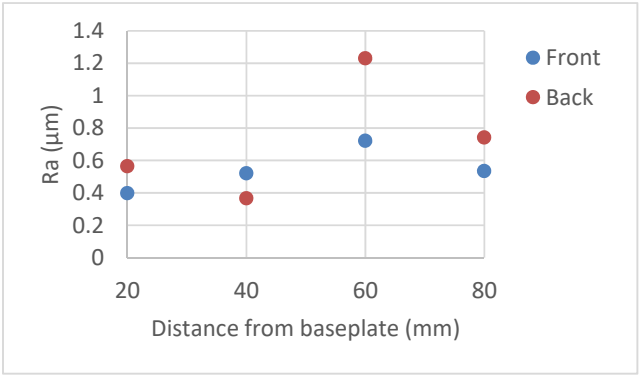

Fig. 15. Average roughness values from wall sides using a stylus profilometer.

The wall dynamics after machining were also of interest. This is another important aspect of the part's digital twin. While geometry and surface finish are important outcomes of machining processes, structural dynamics are also often critical for part performance in its intended application. The results of a wall tap test at the upper corner in the X (flexible) direction are shown in Fig. 16. Two bending modes are observed at 870 Hz and 2193 Hz for the measured frequency range. The mode shape for the lower (first) frequency was identified using direct and cross tap testing data for a grid of points in the YZ plane. A comparison with simulated results from finite element analysis (FEA) of the CAD model is provided in Fig. 17. The results of the tap test and simulation agree.

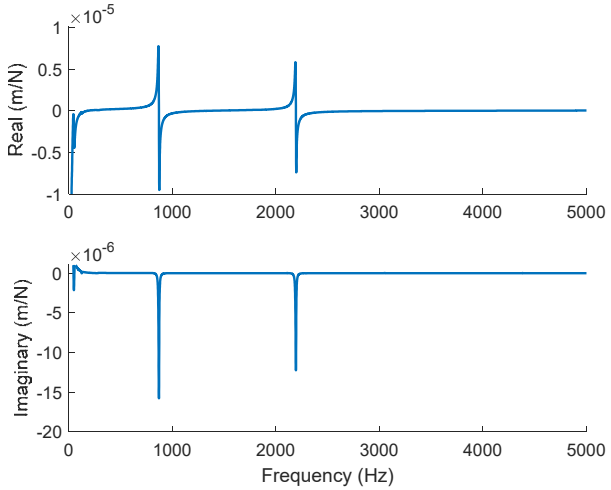

Fig. 16. Real (top panel) and imaginary (bottom panel) parts of the machined wall FRF for the X direction (wall flexible direction).

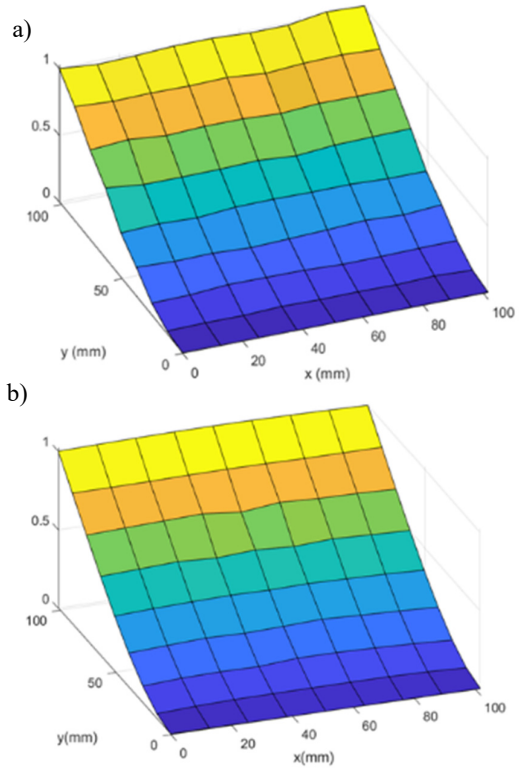

Fig. 17. (a) First mode shape of machined wall from tap testing data; (b) First mode shape of machined wall from finite element analysis.

7. Discussion

This work demonstrates the value of a digital twin for machining operations in hybrid manufacturing. The combination of the fiducial apparatus and structured light scanning provide not only an accurate stock model, but also a connection between the preform and machine coordinate systems. This reduces setup time on the CNC machining center, confirms that the desired part geometry is contained within the as-printed preform for the machining orientation, and enables accurate CAM simulation of the toolpaths using the actual preform geometry.

Measurement of the preform and tool tip FRFs enables selection of machining parameters that provide stable cutting conditions which respect the limitations imposed by the process dynamics, while obtaining the highest possible metal removal rate and, therefore, highest process efficiency. Similarly, by considering the preform dynamics, the initial preform design can be informed (or modified) to ensure that the preform does not significantly reduce metal removal rates due to low dynamic stiffness. This can be a natural outcome of "too-near-net" shape designs.

While measuring the preform and tool tip dynamics enables the pre-process selection of stable cutting parameters with high productivity, tool wear and measurement uncertainties can lead to uncertainty in the stability map. Therefore, in-process signals, such as the audio signal during machining, can serve to augment the predictions and identify unwanted outcomes, such as chatter.

Post-machining part measurements are used to confirm that the intended geometry, surface finish, and dynamics are achieved. In this case, a stylus profilometer was used, although optical methods are also available. Tap testing is used to identify natural frequencies, modal stiffness and damping ratio values, and mode shapes of the machined part. FEA comparisons may also be completed.

Collectively, these components form the machining digital twin for hybrid manufacturing. Further work to evaluate this digital twin methodology will include increasingly complex preform and CAD model geometries, as well as repeatability and reproducibility. This will test the robustness of the methodology while providing further detail on the "manual" step of aligning the stock model and CAD model.

8. Conclusions

In this paper, multiple facets of a machining digital twin for hybrid manufacturing were shown. Temporary fiducials were attached to a WAAM preform and scanned using structured light to define a local coordinate system and CAM stock model. The scan represents a digital twin for the AM geometry and enabled the part to be located in the machine tool using standard probing cycles. The WAAM preform and tool were tap tested to generate a stability map for the machining process, which enabled milling parameter selection, including axial and radial depths of cut, spindle speed, and feed per tooth. The measurement data and models provided a digital twin for the process performance; this information augments the geometry-based CAM description with a physics-based approach for parameter selection. Audio data was recorded during machining and surface profilometry was completed post-machining to validate the absence of chatter and desired surface finish. This data provides a digital twin for the milling process that can be used to distinguish between stable and unstable (chatter) conditions for later reference. A structured light scan of the final part was completed to compare to the CAD model, surface finish measurements were performed, and dynamic testing was performed to identify the vibration response. These geometry, surface finish, and structural dynamics data give the digital twin for the part performance and agreement (or disagreement) with the design intent. The proposed machining digital twin methodology is deemed successful in accurately modeling the machining process and outcome.

Acknowledgements

This work relates to Department of Navy award (ONR Award No. N00014-20-1-2836) issued by the Office of Naval Research. The United States Government has a royalty-free license throughout the world in all copyrightable material contained herein.

This manuscript has been funded by UT-Battelle, LLC, under contract DE-AC05-00OR22725 with the US Department of Energy (DOE). The US government retains and the publisher, by accepting the article for publication, acknowledges that the US government retains a nonexclusive, paid-up, irrevocable, worldwide license to publish or reproduce the published form of this manuscript, or allow others to do so,

for US government purposes. DOE will provide public access to these results of federally sponsored research in accordance with the DOE Public Access Plan (http://energy.gov/downloads/doe-public-access-plan).

References

[1] Tuegel, E.J., Ingraffea, A.R., Eason, T.G. and Spottswood, S.M., 2011. Reengineering aircraft structural life prediction using a digital twin. International Journal of Aerospace Engineering, 2011.

[2] Shafto, M., Conroy, M., Doyle, R., Glaessgen, E., Kemp, C., LeMoigne, J. and Wang, L., 2012. Modeling, simulation, information technology & processing roadmap. National Aeronautics and Space Administration, 32, pp.1-38.

[3] Grieves, M., 2014. Digital twin: manufacturing excellence through virtual factory replication. White paper, 1, pp.1-7.

[4] Boschert, S. and Rosen, R., 2016. Digital twin—the simulation aspect. In Mechatronic futures (pp. 59-74). Springer, Cham.

[5] Negri, E., Fumagalli, L. and Macchi, M., 2017. A review of the roles of digital twin in CPS-based production systems. Procedia Manufacturing, 11, pp.939-948.

[6] Qi, Q. and Tao, F., 2018. Digital twin and big data towards smart manufacturing and industry 4.0: 360 degree comparison. IEEE Access, 6, pp.3585-3593.

[7] Kritzinger, W., Karner, M., Traar, G., Henjes, J. and Sihn, W., 2018. Digital Twin in manufacturing: A categorical literature review and classification. IFAC-PapersOnLine, 51(11), pp.1016-1022.

[8] Tao, F., Zhang, H., Liu, A. and Nee, A.Y., 2018. Digital twin in industry: State-of-the-art. IEEE Transactions on Industrial Informatics, 15(4), pp.2405-2415.

[9] Schmitz, T. and Smith, K.S., 2019, Machining Dynamics: Frequency Response to Improved Productivity, Second Edition, Springer, New York, NY.

[10] Webster, S., Lin, H., Carter, F., Ehmann, K. and Cao, J., 2021. Physical mechanisms in hybrid additive manufacturing: A process design framework. Journal of Materials Processing Technology, p.117048.

[11] Liou, F., Slattery, K., Kinsella, M., Newkirk, J., Chou, H.N. and Landers, R., 2007. Applications of a hybrid manufacturing process for fabrication of metallic structures. Rapid Prototyping Journal, 13(4), pp.236-244.

[12] Yamazaki, T., 2016. Development of a hybrid multi-tasking machine tool: Integration of additive manufacturing technology with CNC machining. Procedia CIRP, 42, pp.81-86.

[13] Song, Y., Park, S., Choi, D., and Jee, H., 2005. 3D welding and milling: Part I-a direct approach for freeform fabrication of metallic prototypes. International Journal of Machine Tool and Manufacture, 45(9), pp.1057-1062.

[14] Xu, J., Xi, N., Zhang, C., Shi, Q., and Gregory, J., 2011. Real-time 3D shape inspection system of automotive parts based on structured light pattern. Optics & Laser Technology, 43(1), pp.1-8.

[15] Mendricky, R., 2016. Determination of measurement accuracy of optical 3D scanners. MM Science Journal, 2016, pp.1565-1572.

[16] Srinivasan, H., Harrysson, O., Wysk, R., 2015. Automatic part localization in a CNC machine coordinate system by means of 3D scans. The International Journal of Advanced Manufacturing Technology, 81, pp.1127-1138.

[17] Woody, B., Smith, S., Hocken, R., and Miller, J., Uncertainity Analysis for the Fiducial Calibration System. Proceedings of the ASME 2005 International Mechanical Engineering Congress and Exposition. Manufacturing Engineering and Materials Handling, Parts A and B. pp.699-706.

[18] Wang, S., Cheung, B., and Ren, M., 2020. Uncertainty analysis of a fiducial-aided calibration and positioning system for precision manufacturing of optical freeform optics. Measurement Science and Technology, 31(6).

[19] Smith, S., Woody, B. A., and Miller, J. A. , 2005. Improving the accuracy of large scale monolithic parts using fiducials, Annals of the CIRP, 56(1): 483-487.

[20] Woody, B.A., Scott Smith, K., Hocken, R.J. and Miller, J.A., 2007. A technique for enhancing machine tool accuracy by transferring the metrology reference from the machine tool to the workpiece. J. Manuf. Sci. Eng., 129(3): 636-643.

[21] Cornelius, A., Dvorak, J., Jacobs, L., Penney, J. and Schmitz, T., 2021. Combination of structured light scanning and external fiducials for coordinate system transfer in hybrid manufacturing. Journal of Manufacturing Processes, 68, pp.1824-1836.

[22] Luo, W., Hu, T., Zhang, C. and Wei, Y., 2019. Digital twin for CNC machine tool: modeling and using strategy. Journal of Ambient Intelligence and Humanized Computing, 10(3), pp.1129-1140.

[23] Zhou, G., Zhang, C., Li, Z., Ding, K. and Wang, C., 2020. Knowledge-driven digital twin manufacturing cell towards intelligent manufacturing. International Journal of Production Research, 58(4), pp.1034-1051.

[24] Smith, S.T., Chetwynd, DG., 1992. Foundations of Ultraprecision Mechanism Design. Gordon and Breach Science Publishers, Belgium.